Lecture 17

Inner Layer Solution

(Text from Bellan)

y-dependence 90° out of phase with respect to the y-direction periodicity of the bars. In particular, there is an outward x-directed velocity at the y location of the O-points and an inward x-directed velocity at the y location of the X-points. The fluid motion thus consists of a spatially periodic set of vortices that are antisymmetric with respect to $x = 0$. Each bar has a pair of opposite vortices for positive x and a mirror image pair of vortices for negative x, so there are four vortices for each bar.

12.4 Semi-quantitative estimate of the tearing process

An exact, self-consistent description of tearing and reconnection is beyond the capability of standard analytic methods because of the multi-scale nature of this process. However, the essential features (geometry, critical parameters, growth rate) and a reasonable physical understanding can be deduced using a semi-quantitative analysis, which outlines the basic physics and determines the relevant orders of magnitude. The starting point for this analysis involves solving for the vector potential associated with the magnetic field in Eq. (12.3), obtaining

$$A_z(x) = -\int^x B_y(x')dx' = -BL\ln\left[\cosh(x/L)\right] + const. \tag{12.9}$$

The constant is chosen to give $A_z = 0$ at $x = 0$ so

$$A_z(x) = -BL\ln\left[\cosh(x/L)\right]. \tag{12.10}$$

For $|x| \ll L$, $\cosh(x/L) \simeq 1 + x^2/L^2$ while for $|x| \gg L$, $\cosh(x/L) \simeq \exp(|x|/L)/2$. Thus, the limiting forms of the vector potential are

$$\lim_{|x|\ll L} A_z(x) = -\frac{Bx^2}{L} \tag{12.11}$$

and

$$\lim_{|x|\gg L} A_z(x) = -BL\left(\frac{|x|}{L} - \ln 2\right). \tag{12.12}$$

Near $x = 0$, A_z is an inverted parabola with a maximum value of zero, while far from $x = 0$, A_z is linear and becomes more negative with increasing displacement from $x = 0$. This behavior of the vector potential is consistent with the field being uniform far from $x = 0$, but reversing sign on going across $x = 0$. The behavior is also consistent with the relationship between the current density and the second derivative of the vector potential,

$$\mu_0 J_z = \frac{\partial B_y}{\partial x} = -\frac{\partial^2 A_z}{\partial x^2}. \tag{12.13}$$

Current density is therefore associated with curvature in $A_z(x)$ or, in a more extreme form, with a discontinuity in the first derivative of $A_z(x)$. Specifying the vector potential is sufficient to characterize the problem since the magnetic field and currents are the first and second derivatives of $A_z(x)$ respectively. This general idea can be extended to more complicated geometries if there is sufficient symmetry so that specification of an equilibrium flux profile uniquely gives both the equilibrium field and the current distribution.

The reconnection process is characterized by the MHD equation of motion

$$\rho\frac{d\mathbf{U}}{dt} = \mathbf{J}\times\mathbf{B} - \nabla P, \tag{12.14}$$

Faraday's law expressed as

$$\mathbf{E} = -\frac{\partial \mathbf{A}}{\partial t}, \tag{12.15}$$

Ampère's law

$$\nabla\times\mathbf{B} = \mu_0\mathbf{J}, \tag{12.16}$$

and the resistive Ohm's law

$$\mathbf{E} + \mathbf{U}\times\mathbf{B} = \eta\mathbf{J}. \tag{12.17}$$

The analysis involves relating the velocity vortices to the linearized Ohm's law, and in particular to its z component

$$E_{z1} + U_{x1}B_{y0} = \eta J_{z1}. \tag{12.18}$$

The sense of the vortices sketched in Fig. 12.2(c) indicate that the velocity perturbation is uniform in the z direction and U_{x1} is *antisymmetric* with respect to x. Also, since the motion consists of vortices, there is no net divergence of the fluid velocity and so it is reasonable and appropriate to stipulate that the flow is *incompressible* with $\nabla\cdot\mathbf{U} = 0$. Since the perturbed current density is in the z direction, and since for straight geometries the vector potential is parallel to the current density, the perturbed vector potential may also be assumed to be in the z direction. Hence, both equilibrium and perturbed vector potentials are in the z direction and so the total magnetic field is related to the total vector potential by

$$\mathbf{B} = \nabla\times A_z\hat{z} = \nabla A_z\times\hat{z}. \tag{12.19}$$

Equation (12.18) can be recast using Eqs. (12.15) and (12.19) as an *induction equation*,

$$-\frac{\partial A_{z1}}{\partial t} - U_{x1}\frac{\partial A_{z0}}{\partial x} = \eta J_{z1}. \tag{12.20}$$

The current has the form

$$\mu_0 J_z = \hat{z}\cdot\nabla\times\mathbf{B} = \hat{z}\cdot\nabla\times(\nabla\times A_z\hat{z}) = \hat{z}\cdot\nabla\times(\nabla A_z\times\hat{z}) = -\nabla_\perp^2 A_z, \qquad (12.21)$$

where the subscript $\perp$ means perpendicular to $\hat{z}$. Thus, the induction equation becomes

$$\frac{\partial A_{z1}}{\partial t} + U_{x1}\frac{\partial A_{z0}}{\partial x} = \frac{\eta}{\mu_0}\nabla_\perp^2 A_{z1}. \qquad (12.22)$$

To proceed, it is necessary to express the perturbed velocity U_{x1} in terms of A_{z1}; this relation is obtained from the equation of motion.

While we could just plow ahead and manipulate the equation of motion to obtain U_{x1} in terms of A_{z1}, it is more efficient to exploit the incompressibility relation. In two-dimensional hydrodynamics, incompressibility simplifies flow dynamics so that flow is described by two related scalars, the stream-function f and the vorticity Ω. For two-dimensional motion in the $x-y$ plane of interest here, the general incompressible velocity can be expressed as

$$\mathbf{U} = \nabla f\times\hat{z}, \qquad (12.23)$$

since

$$\nabla\cdot\mathbf{U} = \nabla\cdot(\nabla f\times\hat{z}) = \hat{z}\cdot\nabla\times\nabla f = 0. \qquad (12.24)$$

The vorticity is the curl of the velocity and because the velocity lies in the $x-y$ plane, the vorticity vector is in the z direction. The vorticity magnitude Ω is given by

$$\Omega = \hat{z}\cdot\nabla\times\mathbf{U} = \hat{z}\cdot\nabla\times(\nabla f\times\hat{z}) = \nabla\cdot[(\nabla f\times\hat{z})\times\hat{z}] = -\nabla_\perp^2 f, \qquad (12.25)$$

where $\perp$ means perpendicular with respect to z. Given the vorticity, f can be found by solving the Poisson-like Eq. (12.25), and then, knowing f, the velocity can be evaluated using Eq. (12.23). Appropriate boundary conditions must be specified for both f and Ω; these boundary conditions are that the vorticity is antisymmetric in x and is only large in the vicinity of $x = 0$ as indicated in Fig. 12.2(c).

The curl of the equation of motion provides the vorticity evolution and also annihilates ∇P; this elimination of P from consideration is why the vorticity/stream-line method is a more efficient approach than direct solution of the equation of motion.

Let us now solve for U_{1x} following this procedure. The linearized equation of motion is

$$\rho_0\frac{\partial \mathbf{U}_1}{\partial t} = (\mathbf{J}\times\mathbf{B})_1 - \nabla P_1; \qquad (12.26)$$

taking the curl and dotting with $\hat{z}$ gives

$$\begin{aligned}\rho_0\frac{\partial \Omega_1}{\partial t} &= \hat{z}\cdot\nabla\times(\mathbf{J}\times\mathbf{B})_1\\ &= \hat{z}\cdot\nabla\times\left[J_z\hat{z}\times(\nabla A_z\times\hat{z})\right]_1\\ &= \hat{z}\cdot\nabla\times(J_z\nabla A_z)_1\\ &= \hat{z}\cdot(\nabla J_z\times\nabla A_z)_1.\end{aligned} \qquad (12.27)$$

Using Eq. (12.21) this can be written as

$$\frac{\partial \Omega_1}{\partial t} = \frac{1}{\mu_0\rho_0}\hat{z}\cdot\left[\nabla A_z\times\nabla(\nabla_\perp^2 A_z)\right]_1. \qquad (12.28)$$

From Fig. 12.2(c) it is expected that the vortices have significant amplitude only in the vicinity of where the current bars are deforming and that at large $|x|$ there will be negligible vorticity. Thus, it is assumed that the vorticity evolution equation has the following behavior:

1. Inner (tearing/reconnection) region: here it is assumed that the perturbation has much steeper gradients than the equilibrium so

$$\frac{|\nabla(\nabla_\perp^2 A_{z0})|}{|\nabla A_{z0}|} \ll \frac{|\nabla(\nabla_\perp^2 A_{z1})|}{|\nabla A_{z1}|}. \qquad (12.29)$$

This allows Eq. (12.28) to be approximated as

$$\begin{aligned}\frac{\partial \Omega_1}{\partial t} &\simeq \frac{1}{\mu_0\rho_0}\hat{z}\cdot\left[\nabla A_{z0}\times\nabla(\nabla_\perp^2 A_{z1})\right]\\ &= \frac{1}{\mu_0\rho_0}\frac{\mathrm{d}A_{z0}}{\mathrm{d}x}\frac{\partial}{\partial y}(\nabla_\perp^2 A_{z1}),\end{aligned} \qquad (12.30)$$

which shows that J_{z1} crossed with B_{y0} generates vorticity. Since B_{y0} is antisymmetric with respect to x, the vortices have the assumed antisymmetry. Furthermore, because J_{z1} is symmetric with respect to x and localized in the vicinity of $x = 0$ the vortices are localized to the vicinity of $x = 0$.

2. Outer (ideal) region: here $\Omega_1 \simeq 0$ is assumed so Eq. (12.28) becomes

$$\frac{\mathrm{d}A_{z0}}{\mathrm{d}x}\frac{\partial}{\partial y}(\nabla_\perp^2 A_{z1}) - \frac{\partial A_{z1}}{\partial y}\frac{\mathrm{d}^3 A_{z0}}{\mathrm{d}x^3} = 0, \qquad (12.31)$$

which is a specification for A_{z1} in the outer region for a given A_{z0}. Thus, it is effectively assumed that the outer perturbed field is force-free, i.e., $(\mathbf{J}\times\mathbf{B})_1 = 0$. This is consistent with there being no generation of vorticity in the outer region.

The perturbed quantities will now be assumed to have the space-time dependence

$$A_{z1} = A_{z1}(x)e^{iky+\gamma t}$$
$$\Omega_1 = \Omega_1(x)e^{iky+\gamma t} \tag{12.32}$$

so Eq. (12.30) gives the inner region vorticity as

$$\Omega_1 = \frac{1}{\mu_0 \gamma \rho_0}\frac{dA_{z0}}{dx} ik\left(\nabla_\perp^2 A_{z1}\right) = -\frac{1}{\gamma\rho_0}\frac{dA_{z0}}{dx} ikJ_{z1}. \tag{12.33}$$

This satisfies all the geometric conditions noted earlier, namely the antisymmetric dependence on x, the localization near $x=0$, and, consistent with Fig. 12.2(c), a y-periodicity 90° out of phase with the periodicity of J_{z1}.

Using Eq. (12.23), it is seen that

$$U_{x1} = \frac{\partial f_1}{\partial y} = ikf_1. \tag{12.34}$$

The stream-function f_1 is a solution of the Poisson-like system Eq. (12.25) and Eq. (12.33),

$$\frac{\partial^2 f_1}{\partial x^2} - k^2 f_1 = \frac{1}{\gamma\rho_0}\frac{dA_{z0}}{dx} ikJ_{z1}. \tag{12.35}$$

Since the perturbed current peaks at $x=0$ and has a width of the order of ϵ, it may be characterized by the Gaussian profile

$$J_{z1} \simeq \frac{\lambda}{\epsilon\sqrt{\pi}} e^{-x^2/\epsilon^2}, \tag{12.36}$$

where

$$\lambda = \int_{layer} J_{z1}dx \tag{12.37}$$

is the total perturbed current in the tearing layer. The gradient of the vector potential can be written as

$$\frac{dA_{z0}}{dx} = -B_{y0}(x) \simeq -\frac{x}{L}B'_{y0}. \tag{12.38}$$

Assuming that the tearing layer is very narrow gives

$$\frac{\partial^2 f_1}{\partial x^2} \gg k^2 f_1 \tag{12.39}$$

so Eq. (12.35) becomes

$$\frac{\partial^2 f_1}{\partial x^2} = -\frac{B'_{y0}}{\gamma L\rho_0} ik\frac{\lambda}{\epsilon\sqrt{\pi}} xe^{-x^2/\epsilon^2} = \frac{ikB'_{y0}}{2\gamma L\rho_0}\frac{\lambda\epsilon}{\sqrt{\pi}}\frac{d}{dx}e^{-x^2/\epsilon^2}. \tag{12.40}$$

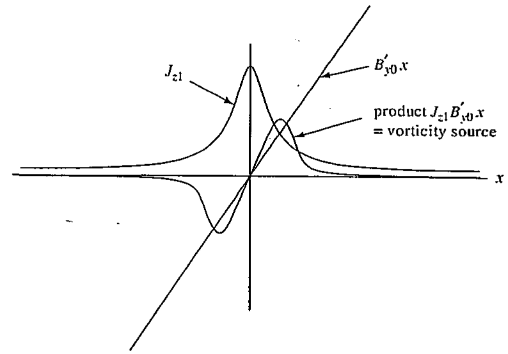

Fig. 12.3 Product of symmetric perturbed current with antisymmetric equilibrium field results in antisymmetric vorticity source localized near $x=0$.

The profiles of J_{z1}, $B_{y0}(x)$, and their product (right-hand side of Eq. (12.40)) are shown in Fig. 12.3.

Integrating Eq. (12.40) with respect to x gives

$$\frac{\partial f_1}{\partial x} = \frac{ikB'_{y0}}{2\gamma L\rho_0}\frac{\lambda\epsilon}{\sqrt{\pi}} e^{-x^2/\epsilon^2}, \tag{12.41}$$

which incidentally gives $U_{1y} = -\partial f_1/\partial x$. Since it is desired to find the magnitude of U_{1x} in the region $x \sim \epsilon$, a rough "order of magnitude" integration of Eq. (12.41) in this region gives

$$f_1 \sim \frac{ikB'_{yo}\lambda\epsilon^2}{2\gamma L\sqrt{\pi}\rho_0} sign(x) \text{ for } x \sim \epsilon \tag{12.42}$$

and so

$$U_{x1} \sim -\frac{k^2 B\lambda\epsilon^2}{2\gamma L\sqrt{\pi}\rho_0} sign(x) \text{ for } x \sim \epsilon. \tag{12.43}$$

The amplitude factor λ can be expressed using Eq. (12.21) as

$$\lambda = -\frac{1}{\mu_0}\int_{layer} \nabla_\perp^2 A_{z1}dx$$
$$\simeq -\frac{1}{\mu_0}\int_{layer} \frac{\partial^2 A_{z1}}{\partial x^2}dx$$
$$= -\frac{1}{\mu_0}\left[\left(\frac{\partial A_{z1}}{\partial x}\right)_+ - \left(\frac{\partial A_{z1}}{\partial x}\right)_-\right], \tag{12.44}$$

where the subscripts $\pm$ mean evaluated at $x = \pm\epsilon$. For purposes of joining to the outer ideal solution, the normalized jump derivative is defined as

$$\Delta' = \frac{\left(\frac{\partial A_{z1}}{\partial x}\right)_+ - \left(\frac{\partial A_{z1}}{\partial x}\right)_-}{A_{z1}(0)} \tag{12.45}$$

so

$$\lambda = -\frac{\Delta'}{\mu_0}A_{z1}(0). \tag{12.46}$$

The velocity becomes

$$U_{x1} \sim \frac{k^2 B\Delta'\epsilon^2}{2\gamma L\sqrt{\pi}\mu_0\rho_0}A_{z1}(0)sign(x) \tag{12.47}$$

and using Eq. (12.36), the current density becomes

$$J_{z1} \sim -\frac{\Delta'}{\epsilon\mu_0\sqrt{\pi}}A_{z1}(0). \tag{12.48}$$

We now repeat the induction equation, Eq. (12.20),

$$-\frac{\partial A_{z1}}{\partial t} - U_{x1}\frac{\partial A_{z0}}{\partial x} = \eta J_{z1} \tag{12.49}$$

and substitute for U_{x1}, J_{z1} and assume that $\partial A_{z0}/\partial x = -B_{y0} \simeq -B\epsilon/L$ in the tearing layer. This gives

$$\underset{\#1}{\gamma} - \underset{\#2}{\frac{k^2B^2\Delta'\epsilon^3}{2\gamma L^2\sqrt{\pi}\mu_0\rho_0}} = \underset{\#3}{\frac{\eta\Delta'}{\epsilon\mu_0\sqrt{\pi}}}, \tag{12.50}$$

where the terms have been numbered for reference in the following discussion.

In the ideal plasma limit, terms #1 and #2 balance each other while term #3 is small; this gives the frozen-in condition. At exactly $x = 0$, term #2 vanishes and so terms #1 and #3 must balance each other, resulting in diffusion of the magnetic field. At the edge of the tearing layer, i.e., at the transition from the ideal limit to the diffusive limit, *all three terms are of the same size.* Thus, the three terms may be equated; this gives two equations that may be solved for γ and ϵ with Δ' as a parameter (Furth, Killeen, and Rosenbluth 1963). Equating terms #1 and #3 gives

$$\gamma = \frac{\eta\Delta'}{\epsilon\mu_0\sqrt{\pi}} \tag{12.51}$$

while equating terms #2 and #3 gives

$$\gamma = \frac{(kB')^2\epsilon^4}{2\eta\rho_0}, \tag{12.52}$$

where $B' = B/L$ is the derivative of the equilibrium field at $x = 0$. Equating these last two equations to eliminate γ gives the width of the tearing layer to be

$$\epsilon \simeq \left[\frac{2\eta^2\rho_0\Delta'}{\mu_0\sqrt{\pi}(kB')^2}\right]^{1/5} \sim \delta_{skin}^{4/5} \tag{12.53}$$

Substituting ϵ back into Eq. (12.51) gives

$$\gamma = 0.55\,(\Delta')^{4/5}\left[\frac{\eta}{\mu_0}\right]^{3/5}\left[\frac{(kB')^2}{\rho_0\mu_0}\right]^{1/5}. \tag{12.54}$$

This result can be put in a more physically intuitive form by defining characteristic times for ideal processes and for resistive processes. The characteristic time for ideal processes is the Alfvén time τ_A, defined as the time to move the characteristic length L when traveling at the Alfvén velocity, i.e.,

$$\tau_A^{-1} = \frac{v_A}{L} = \frac{\sqrt{B^2/\rho_0\mu_0}}{L} = \sqrt{\frac{(B')^2}{\rho_0\mu_0}}. \tag{12.55}$$

The Alfvén time is the characteristic time of ideal MHD and is typically a very fast time. The characteristic time for resistive processes τ_R is defined as the time to diffuse resistively a distance L, so

$$\tau_R^{-1} = \frac{\eta}{L^2\mu_0}. \tag{12.56}$$

For nearly ideal plasmas the resistive time scale is very slow. Using these definitions, Eq. (12.54) can be written as (Furth, Killeen and Rosenbluth 1963)

$$\gamma = 0.55\,(\Delta' L)^{4/5}(kL)^{2/5}\tau_R^{-3/5}\tau_A^{-2/5}. \tag{12.57}$$

All that is needed now is Δ'. This jump condition is found from Eq. (12.31) which gives the form of A_{z1} in the ideal region outside the tearing layer. This can be expressed as

$$\nabla_\perp^2 A_{z1} + \left[B_{y0}^{-1}\frac{d^2 B_{y0}}{dx^2}\right]A_{z1} = 0, \tag{12.58}$$

which shows that the equilibrium magnetic field acts like a "potential" for the perturbed vector potential "wavefunction." If boundary conditions are specified at large $|x|$ for the perturbed vector potential, then there will typically be a discontinuity in the first derivative of A_{z1} at $x=0$; this discontinuity gives Δ'. The jump depends on the existence of a localized equilibrium current since

$$\frac{d^2B_{y0}}{dx^2} = \mu_0 \frac{dJ_{z0}}{dx}. \tag{12.59}$$

Equation (12.58) must in general be solved numerically.

The main result, as given by Eq. (12.57), is that if $\Delta' > 0$ an instability develops having a growth rate *intermediate* between the fast Alfvén time scale and the slow resistive time scale. Since a nearly ideal plasma is being considered, η is extremely small. The width of the tearing layer is therefore very narrow, since, as shown by Eq. (12.53), this width is proportional to $\eta^{2/5}$.

12.5 Generalization of tearing to sheared magnetic fields

The sheet current discussed above can occur in real situations but is a special case of the more general situation where the equilibrium magnetic field does not have a null, but instead is simply sheared. This means that the equilibrium magnetic field is straight, has components in both the y and z directions, and has a direction that is a varying function of x. The sheared situation thus has a uniform magnetic field in the z direction and, instead of the current being concentrated in a sheet, there is simply a non-uniform $B_{y0}(x)$.

There is a non-trivial difference between the special field-null equilibria and the more general types of equilibria where there is no field null. This difference occurs because equilibria involve balancing the magnetic and hydrodynamic pressures in such a way that $P+B^2/2\mu_0$ is continuous within the plasma and also across the plasma boundary. If a field null exists, then equilibrium consists of magnetic pressure $B^2/2\mu_0$ exterior to the null balancing hydrodynamic pressure P at the null and so a reconnection region involving a field null must have $\beta \simeq 1$. This situation occurs in the reconnection region associated with the Earth's magnetotail and has also been studied in certain laboratory plasma experiments (Trintchouk *et al.* 2003). However, in the more general case where there is no field null, B^2 is nearly continuous across the reconnection layer. This means that P will be small, in which case $\beta \ll 1$. Thus, the assumption of low β precludes the possibility of a field null and so precludes the possibility of the simple current sheet discussed in the previous section.

The more general situation where the equilibrium magnetic field has the form

$$\mathbf{B}_0 = B_{y0}(x)\hat{y} + B_{z0}\hat{z} \tag{12.60}$$

would thus be appropriate for low-β plasmas such as tokamaks, spheromaks, and the solar corona. A non-trivial feature of this situation is that, unlike the previously considered sheet current equilibrium, here $B_{y0}(x)$ does not vanish at any particular x. Instead, as will be seen later, what matters is the vanishing of $\mathbf{k}\cdot\mathbf{B}_0$. Equation (12.60) can be used as a slab representation of the straight cylindrical geometry equilibrium field

$$\mathbf{B}_0 = \nabla\psi_0(r) \times \nabla z + B_{z0}\hat{z}. \tag{12.61}$$

Equation (12.61) in turn can be thought of as the straight cylindrical approximation of a toroid with z corresponding to the toroidal angle (see Eq. (9.34)).

Figure 12.4 shows the magnetic field given by Eq. (12.60) as viewed in the $x=0$ plane. In the sheet current analysis discussed in the previous section, the perturbed vector potential pointed in the z direction and was periodic in the y direction. This corresponded to having $\mathbf{k}\cdot\mathbf{A}_1 = 0$ so that the wavevector was orthogonal to the vector potential and both were orthogonal to x. Other important properties were that $\mathbf{k}\cdot\mathbf{B}$ vanished at the reconnection layer, the fluid vorticity vector was pointed in the z direction, the perturbed currents and perturbed magnetic fields were such that $J_1/J_0 \gg B_1/B_0$ in the reconnection layer, and $J_1/J_0 \sim B_1/B_0$ in the exterior region.

These relationships and approximations are generalized here and, in particular, it is assumed all perturbed quantities have functional dependence $\sim g(x)\exp(ik_y y + ik_z z + \gamma t)$. As before, the vorticity equation is the curl of the linearized equation of motion, i.e.,

$$\rho_0 \frac{\partial \Omega_1}{\partial t} = \nabla \times (\mathbf{J}_1 \times \mathbf{B}_0 + \mathbf{J}_0 \times \mathbf{B}_1) \tag{12.62}$$

and in the reconnection layer where $J_1/J_0 \gg B_1/B_0$ this becomes

$$\begin{aligned} \rho_0 \frac{\partial \Omega_1}{\partial t} &= \nabla \times (\mathbf{J}_1 \times \mathbf{B}_0) \\ &= \mathbf{B}_0 \cdot \nabla \mathbf{J}_1 - \mathbf{J}_1 \cdot \nabla \mathbf{B}_0 \end{aligned} \tag{12.63}$$

since $\nabla\cdot\mathbf{B}_0 = 0$ and $\nabla\cdot\mathbf{J}_1 = 0$.

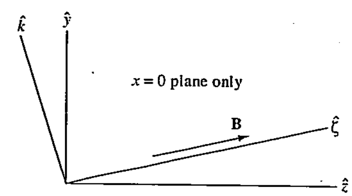

Fig. 12.4 Tilted coordinate system for general sheared field.

An essential feature of the reconnection topology is that the vorticity must be antisymmetric about the reconnection layer, as can be seen from examination of the fluid flow vectors in Fig. 12.2(c). Since the vorticity is created by the torque (i.e., the curl of the force), it is clear that the torque must be antisymmetric about the reconnection layer. As will be seen in the next paragraphs, the condition that the torque is antisymmetric does not imply that either $\mathbf{B}_0$ or $\mathbf{J}_1$ are antisymmetric, but rather implies some more subtle conditions.

Thus, if $x=0$ is defined to be the location of the reconnection layer, then Ω_1 must be an odd function of x and therefore must vanish at $x=0$. Hence, the right-hand side of Eq. (12.63) must vanish at $x=0$ and, since there need be no particular functional relationship between $\mathbf{B}_0$ and its gradient, the two terms on the right-hand side of Eq. (12.63) must separately vanish. Therefore, one of the requirements is to choose the origin of the x axis such that $\mathbf{B}_0\cdot\nabla\mathbf{J}_1=0$ at $x=0$ or, equivalently,

$$\mathbf{k}\cdot\mathbf{B}_0=0 \text{ at } x=0 \tag{12.64}$$

so that

$$k_yB_{y0}(0)+k_zB_{z0}=0. \tag{12.65}$$

Having $\mathbf{k}\cdot\mathbf{B}$ vanish at the reconnection layer is physically reasonable, since finite $\mathbf{k}\cdot\mathbf{B}$ implies a periodic bending of the equilibrium field; such a bending absorbs energy and so is stabilizing. Having $\mathbf{k}\cdot\mathbf{B}$ vanish is like letting the instability cleave the system at a weak point so the instability can develop without requiring much free energy.

The second requirement for the right-hand side of Eq. (12.63) to vanish is to have $\mathbf{J}_1\cdot\nabla\mathbf{B}_0=0$. If the flow is incompressible, then the perturbed magnetic field must be orthogonal to the equilibrium magnetic field and since the perturbed current is the curl of the perturbed magnetic field, the perturbed current must be parallel to the equilibrium magnetic field (this is essentially shear Alfvén wave physics). Since $\mathbf{B}_0$ is assumed straight, $\mathbf{B}_0\cdot\nabla\mathbf{B}_0=0$ and, since $\mathbf{J}_1$ is parallel to $\mathbf{B}_0$, it is seen that $\mathbf{J}_1\cdot\nabla\mathbf{B}_0=(J_1/B_0)\,\mathbf{B}_0\cdot\nabla\mathbf{B}_0=0$. Because $\mathbf{J}_1$ is parallel to $\mathbf{B}_0$, $\mathbf{J}_1$ must also be straight and so a Coulomb gauge vector potential will be parallel to $\mathbf{J}_1$, since

$$\begin{aligned}\mu_0\mathbf{J}_1&=\nabla\times\nabla\times\mathbf{A}_1\\&=\nabla\nabla\cdot\mathbf{A}_1-\nabla^2\mathbf{A}_1\\&=-\nabla^2\mathbf{A}_1\\&=-\hat{\zeta}\nabla^2\mathbf{A}_1\end{aligned} \tag{12.66}$$

can be satisfied by having both $\mathbf{J}_1$ and $\mathbf{A}_1$ in the direction of $\hat{\zeta}$, where $\hat{\zeta}=\mathbf{B}_0(0)/B_0(0)$ does not depend on position.

It is therefore assumed that $\mathbf{A}_1$ is parallel to $\mathbf{B}_0(0)$ and so

$$\mathbf{A}_1(x,y,z,t)=A_{1\zeta}(x)\hat{\zeta}e^{ik_yy+ik_zz+\gamma t}. \tag{12.67}$$

Thus, $\mathbf{k}\cdot\mathbf{A}_1=0$ in this tilted coordinate system since $\mathbf{k}\cdot\hat{\zeta}=\mathbf{k}\cdot\mathbf{B}_0(0)/|\mathbf{B}_0(0)|$. Also $\nabla\cdot\mathbf{A}_1=0$ so the Coulomb gauge assumption is satisfied.

Reconsideration of the right-hand side of Eq. (12.63) shows that although the two terms both vanish at $x=0$ there is a difference in the geometrical dependence of these terms. In particular, since $\mathbf{J}_1$ is in the $\hat{\zeta}$ direction, it has no x component, whereas $\mathbf{B}_0$ depends only on x so

$$\mathbf{J}_1\cdot\nabla\mathbf{B}_0=\left(J_{y1}\frac{\partial}{\partial y}+J_{z1}\frac{\partial}{\partial z}\right)\mathbf{B}_0(x)=0. \tag{12.68}$$

Thus, Eq. (12.63) reduces to

$$\begin{aligned}\rho\frac{\partial\Omega_1}{\partial t}&=\mathbf{B}_0\cdot\nabla\mathbf{J}_1\\&=i\,(\mathbf{k}\cdot\mathbf{B}_0)\,\mathbf{J}_1,\end{aligned} \tag{12.69}$$

where, by assumption, $\mathbf{k}\cdot\mathbf{B}_0$ vanishes at $x=0$.

Continuing this discussion of the ramifications of the antisymmetry of $\mathbf{k}\cdot\mathbf{B}_0$ about $x=0$, we now define an artificial reference magnetic field $\bar{\mathbf{B}}$ that is parallel to the real field at $x=0$, but has no shear (i.e., has no x dependence). The reference field therefore has the form

$$\bar{\mathbf{B}}=B_{y0}(0)\hat{y}+B_{z0}\hat{z}=B_0(0)\hat{\zeta} \text{ for all values of } x. \tag{12.70}$$

We now define $\mathbf{b}_0(x)$ as the difference between the real field and $\bar{\mathbf{B}}$ so that

$$\mathbf{B}_0(x)=\bar{\mathbf{B}}+\mathbf{b}_0(x). \tag{12.71}$$

Thus $\mathbf{b}_0(x)$ has the same x dependence as the B_{y0} field used for the sheet current instability in the previous section in that (i) it is antisymmetric about x and (ii) it is in the y direction. One way of thinking about this is to realize that $\mathbf{b}_0(x)$ is the component of $\mathbf{B}_0(x)$ that is antisymmetric about $x=0$. With this definition

$$\mathbf{k}\cdot\mathbf{B}_0=\mathbf{k}\cdot\mathbf{b}_0(x)=k_yb_0 \tag{12.72}$$

and so Eq. (12.69) becomes

$$\gamma\rho_0\Omega_{\zeta1}=ik_yb_0J_{\zeta1}. \tag{12.73}$$

This equation provides the essence of the dynamics. It shows how the component of the magnetic field that is antisymmetric about $x=0$ creates fluid vortices that are antisymmetric with respect to x. In particular, since $\mathbf{b}_0(x)$ is an odd function of x and $J_{\zeta1}$ is an even function of x, $\Omega_{\zeta1}$ is an odd function of x.

The complete self-consistent description is obtained by, in addition, taking into account the induction equation, which shows how fluid motion acts to create perturbations of the electromagnetic field.

In the sheet current case the component of Ohm's law in the direction of symmetry of the perturbation was considered, i.e., the component in the z direction. Here, the corresponding symmetry direction for the perturbation is the ζ direction and so the relevant component of Ohm's law is the ζ component,

$$\hat{\zeta}\cdot[\mathbf{E}_1+\mathbf{U}_1\times\mathbf{B}_0(x)]=\hat{\zeta}\cdot\eta\mathbf{J}_1, \tag{12.74}$$

which becomes

$$-\frac{\partial A_{\zeta 1}}{\partial t}+\left(\hat{y}\times\hat{\zeta}\cdot\mathbf{U}_1\right)b_0(x)=\eta J_{\zeta 1}. \tag{12.75}$$

Since the vorticity vector lies along $\hat{\zeta}$, the incompressible velocity must be orthogonal to $\hat{\zeta}$ and so has the form

$$\mathbf{U}_1=\nabla f_1\times\hat{\zeta}. \tag{12.76}$$

Thus,

$$\hat{y}\times\hat{\zeta}\cdot\mathbf{U}_1=\left(\hat{y}\times\hat{\zeta}\right)\cdot\left(\nabla f_1\times\hat{\zeta}\right)=ik_y f_1. \tag{12.77}$$

Taking into account the ζ direction of the vorticity once again, it is seen that $\Omega_1=\Omega_{\zeta 1}\hat{\zeta}$, where

$$\Omega_{\zeta 1}=\hat{\zeta}\cdot\nabla\times\mathbf{U}_1=-\nabla_\perp^2 f_1 \tag{12.78}$$

and now $\perp$ means perpendicular to $\hat{\zeta}$.

Substituting for $\Omega_{\zeta 1}$ in Eq. (12.73) using Eq. (12.78) gives

$$\nabla_\perp^2 f_1=-\frac{ik_y b_0(x)J_{\zeta 1}}{\gamma\rho_0}; \tag{12.79}$$

this equation provides the essential dynamics of fluid vortices that are antisymmetric with respect to x and driven by the torque associated with the non-conservative $\mathbf{J}\times\mathbf{B}$ force. This is essentially the same as Eq. (12.35) and the rest of the analysis is the same as for the sheet current problem except that now k_y is used instead of k and b_0' is used instead of B_{y0}' since $b_0(x)$ only differs from $B_{y0}(x)$ by a constant, $b_0'=B_{y0}'$. Thus, using Eq. (12.54) the growth rate will be

$$\gamma=0.55\left(\Delta'\right)^{4/5}\left[\frac{\eta}{\mu_0}\right]^{3/5}\left[\frac{\left(k_yB_{y0}'\right)^2}{\rho_0\mu_0}\right]^{1/5}. \tag{12.80}$$

The global system has to be periodic in both the y and z direction in order for well-defined k_y and k_z to exist. In particular, the physical arrangement and

dimensions of the global system determine the quantized spectra of k_y and k_z and so determine the allowed planes where $\mathbf{k}\cdot\mathbf{B}_0$ can vanish. As suggested earlier, the allowed planes can be considered as "cleavage" planes where the magnetic field can most easily become unglued from the plasma.

Let us express this result in the context of toroidal geometry such as that of a tokamak. This is done by letting B_{z0} correspond to the toroidal field B_ϕ and B_y correspond to B_θ the poloidal field. The Alfvén time is now defined in terms of B_ϕ as

$$\tau_A^{-1}=\frac{B_\phi}{a\sqrt{\rho_0\mu_0}}, \tag{12.81}$$

where a is the minor radius. The safety factor, a measure of the twist, is defined as

$$q=\frac{aB_\phi}{RB_\theta} \tag{12.82}$$

so

$$B_\theta=\frac{aB_\phi}{Rq} \tag{12.83}$$

and

$$B_{y0}'\to-\frac{aB_\phi}{Rq^2}q'. \tag{12.84}$$

Thus, it is possible to replace $k_y\to m/a$ and

$$\frac{\left(k_yB_{y0}'\right)^2}{\rho_0\mu_0}\to\left(\frac{ma}{Rq^2}q'\right)^2\frac{1}{\tau_A}. \tag{12.85}$$

At the tearing layer $\mathbf{k}\cdot\mathbf{B}=0$ or

$$\frac{m}{a}B_\theta+\frac{n}{R}B_\phi=0 \tag{12.86}$$

so

$$q=-\frac{m}{n} \tag{12.87}$$

and Eq. (12.85) becomes

$$\frac{\left(k_yB_{y0}'\right)^2}{\rho_0\mu_0}\to\left(\frac{na}{R}\frac{q'}{q}\right)^2\frac{1}{\tau_A}. \tag{12.88}$$

Thus, Eq. (12.80) becomes

$$\gamma=0.55\left(\Delta'a\right)^{4/5}\tau_R^{-3/5}\tau_A^{-2/5}\left(\frac{na^2}{R}\frac{q'}{q}\right)^{2/5}, \tag{12.89}$$

where

$$\tau_R^{-1} = \frac{\eta}{a^2\mu_0}. \qquad (12.90)$$

Equation (12.89) shows that the essential source for the tearing instability is q'. From this point of view, the "free energy" is in the gradient of q and so, as the tearing mode uses up this free energy, the q profile will be flattened. The concept that gradients in q drive reconnection is closely related to the concept that relaxation is driven by gradients in the force-free parameter λ discussed with regards to Eq. (10.140). This is because λ is essentially the axial current I flowing through a flux tube with flux Φ. This can be seen by integrating Eq. (10.140) over the cross-section of a current-carrying flux tube to obtain

$$\frac{\mu_0 I}{\Phi} = \frac{\int \nabla\times\mathbf{B}\cdot d\mathbf{s}}{\int \mathbf{B}\cdot d\mathbf{s}} = \lambda. \qquad (12.91)$$

If the torus is approximated as a straight cylinder so B_ϕ is the axial field and $B_\theta = \mu_0 I/2\pi a$ is the azimuthal field then the axial flux is $\Phi = \pi a^2 B_\phi$ and

$$q = \frac{aB_\phi}{RB_\theta} = \frac{2\pi a^2 B_\phi}{R\mu_0 I} = \frac{2\Phi}{R\mu_0 I}. \qquad (12.92)$$

We see that

$$q = \frac{2}{\lambda R} \qquad (12.93)$$

so

$$q' = -\frac{2}{\lambda^2 R}\lambda'. \qquad (12.94)$$

Thus, q and λ are inversely related and the concept that gradients in λ drive instability is essentially equivalent to the concept that gradients in q drive instability.

12.6 Magnetic islands

The tearing instability changes the topology of the magnetic field and causes the formation of magnetic "islands" (Rutherford 1973, Bateman 1978). The equilibrium magnetic field has the form

$$\mathbf{B} = \bar{\mathbf{B}} + b_0(x)\hat{y} = \bar{\mathbf{B}} + xB'_{y0}\hat{y} = \bar{\mathbf{B}} + \hat{z}\times\nabla A_{z0}(x), \qquad (12.95)$$

where

$$A_{z0}(x) = \frac{x^2 B'_{y0}}{2}. \qquad (12.96)$$

It is seen that

$$\mathbf{B}_\perp\cdot\nabla A_{z0} = 0, \qquad (12.97)$$

where $\mathbf{B}_\perp$ is the component perpendicular to z. Thus, the surfaces $A_z = const.$ give the projection of the field lines in the plane perpendicular to z; these projections are the Cartesian geometry equivalents to the poloidal flux surfaces of toroidal geometry.

If it is assumed that $k_z \ll k_y$, so ζ is very nearly parallel to z, then it is seen that the tearing instability adds a perturbation to A_z giving

$$A_z(x, y) = \frac{x^2 B'_{y0}}{2} + A_{z1}\cos k_y y. \qquad (12.98)$$

A sketch of a set of surfaces of constant $A_z(x, y)$ is shown in Fig. 12.5. These surfaces consist of (i) closed curves called islands, (ii) a separatrix that passes through the X-point, and (iii) open outer surfaces. On the $x = 0$ line an O-point corresponds to a maximum in $\cos k_y y$ (e.g., $k_y y = 0$) and an X-point corresponds to a minimum (e.g., $k_y y = \pm\pi$). The maximum width w of the separatrix can be calculated by noting that at the X-point (i.e., where $\cos(k_y y) = 1$ and $x = 0$)

$$A_z = 0 + A_{z1} \qquad (12.99)$$

while at the point of maximum width on the separatrix (i.e., where $\cos(k_y y) = -1$ and $x = w/2$)

$$A_z = \frac{(w/2)^2 B'_{y0}}{2} - A_{z1}. \qquad (12.100)$$

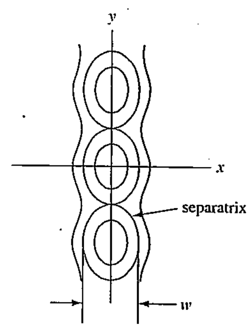

Fig. 12.5 Surfaces of constant A_z showing magnetic islands and separatrix with width w.